Int.J.Curr.Res.Aca.Rev.2024; 12(11): 38-55

EXCELLENT PUBLISHERS

International Journal of Current Research and Academic Review

ISSN: 2347-3215 (Online) Volume 12 Number 11 (November-2024)

Journal homepage: http://www.ijcrar.com

doi: https://doi.org/10.20546/ijcrar.2024.1211.002

Application of X-Ray Diffraction for Mineralogical Composition Studies of Tarat Formation Sandstone in the Tamari Prospect, Northern Niger

Tourba Kamayé[1], Abdou Dodo Bohari[2*], Ibrahim Sarki Laouali[3], Ibrahim Hassan Mahrou[4], Mallam Maman Halarou[5], Hamma Ada Moussa[6] and Moussa Harouna[7]

Niamey, Niger

**Corresponding author*

Abstract

This research work aimed to determine the mineralogical composition of Tarart formation. A total of tens representative samples was subjected to X-Ray Diffraction analysis (XRD) which present nowadays an important and widely used material characterization technique. Three different groups of minerals are distinguished and interpreted. Such as group of clay minerals, group of detrital minerals and group of uranium minerals. The group of clay minerals are mainly composed of chlorite, kaolinite, illite, illite-smectite (I-S) interstratified rocks, and chlorite-smectite (C-S) presented as corrensite. The group of detrital minerals are quartz, feldspar, rutile, calcite and hematite. Uraninite constitutes the group of uranium minerals. The genesis of illite, chlorite and kaolinite are essentially detrital and were formed by the alteration of various sources of parent rocks such as acidic igneous rocks and ancient sedimentary rocks. Illite indicates a siliceous source and the low abundance of kaolinite content testifies to the major predominance of arid climatic conditions in the initial environment of deposition.

Article Info

Received: 15 September 2024
Accepted: 28 October 2024
Available Online: 20 November 2024

Keywords

X-Ray Diffraction, illite-smectite, chlorite-smectite, uraninite, Tarat Formation.

Introduction

The study of the mineralogical composition of fine-grained minerals such as clays and clayey mixed-layered clays is very important because they reflect the mineralogy of the parent rock and the type of alteration affecting these rocks. Also, clay minerals and their abundance record information related to climate, alteration and diagenesis. The type of clay found depends mainly on the interaction of climate, parent rock and depositional environment (Velde, 1995; Bouchet *et al.,* 2000). The distribution of clay minerals in sediments is affected by the detrital input of the sedimentary basin. Clay minerals such as mica, chlorite, associated with quartz and feldspars are typically terrigenous natures (Chamley, 1989; Claret, 2001).

Genetically, minerals are natural chemical compounds and are products of various physicochemical processes occurring in the earth's crust, as well as products of the biological activity of various organisms. The clay minerals commonly found in nature are kaolinite, illite, smectite and chlorite; therefore, clay minerals are essentially attributed to three origins: (i) inheritance, (ii) transformation and (iii) neoformation (Millot, 1964).

The alteration processes linked to argilization in the sandstones of the Tarat formation are at the origin of the phenomena of neoformation and clay and carbonate cementation of sandstones. Several studies (Cavelec, 2006; Billon, 2014 and Mamane, 2016) have been undertaken with the aim of characterizing the

neoformations and clay cementations but also to better understand the detrital heritage and its evolution during the diagenesis of the basin more concretely in the Tamari prospect sector.

The study of these clay minerals requires the use of the X-ray diffraction method (XRD) which is currently the most effective method for determining the mineralogical composition of rocks and especially fine-grained minerals with a complex structure such as clay and uranium minerals generally found in sedimentary rocks (Tucker, 1988, 1991; Moore *et al.,* 1989; Plançon and Drits, 2000).

The aim of this work is mainly the identification of fine-grained minerals such as clays and mixed-layer clays and uranium minerals that are difficult to determine optically and subsequently deduce the origin of these clay minerals.

Location of the study area

The Tamari Sector is located mainly on the Tamou East Amodiation of the Somaïr. It is limited to the East by the Arlequin sector, to the West by the Tamou deposits, to the South by the Tin Adrar beam and to the North by the Arlette and Ariège deposits. The Tamari sector is focused to the East of the Arlit accident (Figure 1). Structurally, the area is surrounded by anticlinal structures and flexures on both sides. An anticline and a flexure towards the West in a North-South direction, the flexure crosses the study sector a little in the middle and the anticline is located on the limits of the old Tamou pit. To the East there is also an anticline and a flexure in NNW-SSE direction (Figure 2).

Geological setting

The geology of northern Niger is dominated by the Air Massif, which is a host block of pre-Cambrian calc-alkaline metamorphic and intrusive rocks, cut by Paleozoic (gabbro)-syenite-granite ring complexes (Figure 3).

The continental intercalaire series (Paleozoic and Mesozoic formations) develops in the Tim-Mersoi basin along the western margin of the Air Massif and includes formations ranging from Cambrian to Cretaceous (Turpin *et al.,* 1991). In the early Paleozoic (Cambrian and Carboniferous periods), sediments began to accumulate in a shallow depression.

The Carboniferous Terada and Tagora series were deposited during this period, the Terada series comprising fluvio-glacial conglomerates and sandstones while the Tagora series is composed of fluvio-deltaic sandstones. Each of these series is intercalated by silt and continental sandstone (Kogbe, 1991).

At the end of the Paleozoic, carbonate began to cement the sediments and gypsum nodules intruded into the clays. While a rare mineral, analcime (feldspathoid with high pH and high concentrations of silica and sodium), formed thin beds in the Jurassic period (Agadez series), carbonates again predominated during the Late Cretaceous. In the middle and late Mesozoic (Jurassic to Cretaceous), highly alkaline volcanic eruptions began north-south about 100 km east of the Tim-Mersoi basin in the Aïr massif (Kogbe, 1991).

The stratigraphic succession of the study area (figure 3) is essentially composed of the Izegwadane, Arlit, Tarat and Thinezogue series. The target formation is the Tarat which contains all the mineralizations recognized on the Tamari subject. The Tarat is essentially formed of terrigenous detrital rocks ranging from fine to coarse sandstones or even micro conglomeratic to black clay-silt deposited in a fluvio-deltaic environment.

The Tarat is rich in organic matter (plants), the base of the formation is very erosive and rests unconformably on the Tchinézogue. At the scale of the Tamari deposit, four sequences or units can be clearly distinguished (Figures 4et 5): Unit 4 (U4) consisting of fine sandstone and alternating clay-silt with reduced character; Unit 3 (U3) presents a facies of reduced heterogranular sandstone ranging from very fine to fine sandstones to coarse to very coarse sandstones at the base; Unit 2 (U2) composed of fine to very fine light grey to grey-white sandstone with kaolin cement and unit (U1) presents a facies of coarse to very coarse sandstone with smoky quartz and impregnation of organic matter and pyrite.

Materials and Methods

Tens representative core samples from TMRI 420_2 were collected and subjected to mechanical treatments (crushing and grinding) at the laboratory of the Department of Geology and Mineral Sciences of the University of Ilorin in Nigeria (Figure 6). During these treatments, necessary precautions were taken to avoid contamination of the samples. X-ray diffraction analysis was carried out at the Department of Mineralogy of AGH University of Science and Technology in Poland and at

the Indian Instrumentation Center of IIT Roorkee, India with PANalytical X'Pert PRO diffractometer with an X'Celerator detector, equipped with a copper anticathode and delivering a voltage of 45kV for an intensity of 40mA.

This diffractometer is also equipped with a nickel filter (source and detector), 0.02 radian solers (incident and diffracted beam), one-quarter divergence slits (incident beam), a 10 mm wide mask, one and a half anti-scattering slits for the incident beam and one-quarter for the diffracted beam (Figure 7).

Randomly oriented powder samples and oriented slides were prepared according to the procedures described by Waseda *et al.,* (2011); Brandt and Kinneging (2005); Butt and Shale (2012); Jesche *et al.,* (2016); Matsubara *et al.,* (2011). They were scanned over the range of 4° to 40° 2θ at a scanning speed of 2° 2θ/mim.

The oriented slides were analyzed in different steps (untreated, treated with ethylene glycol at 60°C / 2hr to distinguish the expansive mineral phases, the slides were heated at 350°C / 2hr and 550°C / 2hr for chlorite detection).

All the basal reflection peaks of the minerals were diagnosed according to the ASTM charts, the semi-quantitative determination of the relative amounts of the main clay minerals was calculated using the PANalytical X'Pert HighScore and X-Rayanam software according to the specific reflections and intensity factors.

The X-ray diffraction method is based on the principle that any crystallized body presents atomic arrangements according to specific crystal planes (Ameh, 2019; Cullity and Stock, 2014; Bish and Reynolds, 2018). The diffraction of an X-ray beam, of wavelength λ and angle of incidence θ, by these crystal planes is carried out according to Bragg's law:

$n\lambda = 2d \sin \theta$

Where n = integer and d = spacing between 2 successive parallel planes of the crystal lattice. A crystal can therefore diffract X-rays but this reflection only occurs for certain values of θ. The identification of the different clay minerals is essentially based on the recognition of the inter-reticular distance of the (001) planes and their harmonics (Ameh, 2019; Cullity and Stock, 2014; Bish and Reynolds, 2018).

In an X-ray diffractometer (Figure 8), the sample is rotated at an angle θ about the axis of the goniometer. The X-ray tube is oriented perpendicular to the axis of the goniometer. The primary beam is filtered to produce monochromatic radiation, and passes through a set of slits before it strikes the sample. The diffracted beam (secondary beam) then passes through another set of slits before reaching the detector. The detector is attached to the goniometer and rotated at twice the sample flow rate. The intensity of the beam received at the detector is recorded as a digital file and displayed as a function of the angle of incidence as peaks on a diffractogram.

Results and Discussion

The mineralogical characterization of the studied sample was based on X-ray diffraction analyses for the claystone and siltstone samples of Tarat Formation. The results of the X-ray analysis (figures 9 to 13), show the presence of three groups of minerals such as clay minerals, detrital minerals and uriniferous mineral.

The different types of minerals associated or not with mineralization are mainly: group of clay minerals, group of detrital minerals and group of uranium minerals. The group of clay minerals are mainly composed of chlorite, kaolinite, illite, illite-smectite (I-S) interstratified rocks, and chlorite-smectite (C-S). These interstratified were called corrensite by Pacquet (1969) and Forbes (1983); Rigault (2010). The group of detrital minerals are quartz, feldspar, rutile, calcite and hematite. Uraninite constitutes the group of uranium minerals (Figures 9-13).

Clay minerals

The clay minerals in the studied formation varied from chlorite, kaolinite, illite, illite-smectite (I-S) interstratified rocks, and chlorite-smectite (C-S)

Chlorite

Chlorite is identified in our samples from the Tarat Formation at basal reflections of 14.22, 7.11, 4.72 and 3.54 which correspond respectively to the lines (001), (002) and (004) (Figures 9-13). The even lines are thin and intense while the odd lines have low intensities. These differences in intensity are attributed to the presence of iron in the chlorite lattice (Billault, 2002). The projection of the results of chemical analysis with the electron microprobe in the ternary diagram 3R2, MR3, 2R3 (Velde, 1985) where the different poles are expressed as follows:

2R3 =(Al+Fe-MR3)/2

3R2= (Mg+Fe+Mn)/3

MR3= K+Na+2Ca

This diagram indicates that the chlorites of the Tarat Formation are mainly trioctahedral (Figure 14). The trioctahedral iron chlorites of the Tarat Formation can be separated into several categories according to the classification of Foster (1962) (Figure 15), this diagram classifies the Tarat chlorites into the species chamosite, brunsvigite, Brunsvigite, Diabantite and Penninite according to the nomenclature of Bailey (1982). In the classification of Curtis *et al.,* (1985) our chlorites of the Tarat Formation which are swelling chlorites (Figure 16).

Chlorite-smectite interstratified layers

The chlorite-smectite interstratification was identified by XRD (Figures 9, 12 and 13). Projection of the electron microprobe analysis data of the chlorite-smectite interstratifications indicate that these interstratified chlorites are dioctahedral to trioctahedral corrensites (Figure 14).

However, many authors (Pacquet, 1969; Billault, 2002; Kindraich and Beaufort, 2008) mention that corrensites are regular 1:1 interstratified rock of trioctahedral chlorite and trioctahedral smectite or vermiculite.

Furthermore, others authors (Pacquet, 1969; Billault, 2002; Kindraich and Beaufort, 2008) apply the term corrensite to all interstratified chlorite/smectite, chlorite/vermiculite, or even chlorite/swelling chlorite, even in the case of non-trioctahedral phases. According to Pacquet (1969); Billault (2002); Kindraich and Beaufort (2008), the dioctahedral corrensites in the Mg-Fe-Al(VI) triangular diagram (Figure 17) are rarely pure but they are associated with chlorites. The projection of C-S analyses into the ternary diagram (MR3-2R3-3R2) of Velde (1985) (Figure 18) shows us a distribution between the theoretical composition of the illite-smectite phase and that of low-charge and high-charge montmorillonite, which would therefore be the components of the interstratified.

Illite

The observed illites were identified by X-ray diffraction at basal reflections 10 Å, 5 Å and 3.33 Å (Figures 9-1A, 10-3A, 11, 12-7A and 13). The illites of the Tarat formation have been described extensively in Chapter VII.

Many analyses carried out with the electron microprobe were carried out on the 3R2-MR3-2R3 triangular diagram of Velde (1985) (Figure 19). These analyses are located in the field of low to high charge montmorillonite. Indeed, illite in its pure form is very rare, it is often associated with low to high charge montmorillonites which make the quantification of clays very difficult.

Illite-smectite interstratified layers

Illite-smectite (I-S) interstratified rocks were identified by XRD (Figures 10, 11 and 13).Electron microprobe analysis data of illite-smectite interstratification projected in the diagram (Figure 20) indicate that illite-smectite interstratified rocks in its pure form are very rare, often associated with illites and montmorillonites.

Kaolinite

Kaolinite is a 1:1 dioctahedral phyllosilicate. It has been recognized by optical and electron microscopy in the form of accordion stacks, hexagonal microplatelets. Kaolinite was identified in almost all of our samples at the following reflections: 7.15, 3.58 Å 7.2 and 3.57 (Figures 9-13).

The projection of the electron microprobe analysis data into the triangular diagram of Velde (1985) distributes our samples in the kaolin field (Figure 21).

Detrital minerals

The detrital minerals encountered are essentially composed of Quartz, Potassium Feldspar, Rutile, Calcite and Hematite.

Quartz

Quartz is the most abundant because it constitutes the bulk of sandstone formations in general and of the detrital fraction in particular. This mineral is detected by X-ray diffraction in almost all of the samples analyzed (Figures9-13).

Potassic Feldspar

Potassic feldspar was highlighted in all samples analyzed by X-ray diffraction (Figures 9-13). They are characterized by weak to very weak peaks with variable rays. This indicates a very high degree of alteration of these minerals in the Tarat formation.

Figure.1 Location of the study area (Areva, 2009)

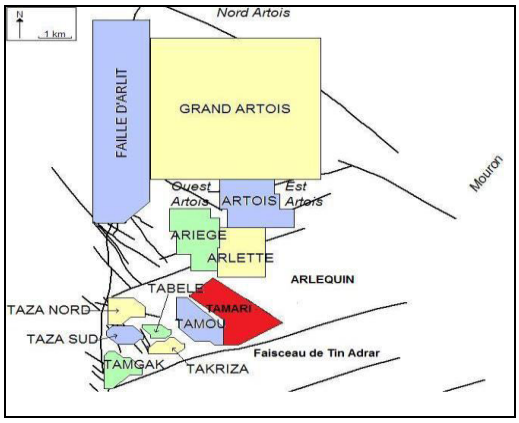

Figure.2 Structural map of the study area (Areva, 2009)

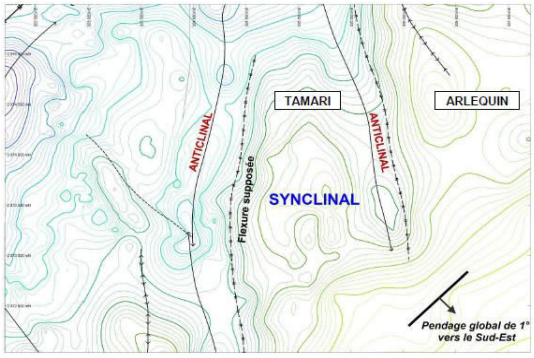

Figure.3 Geological map of northern Niger (modified from Areva, 2009)

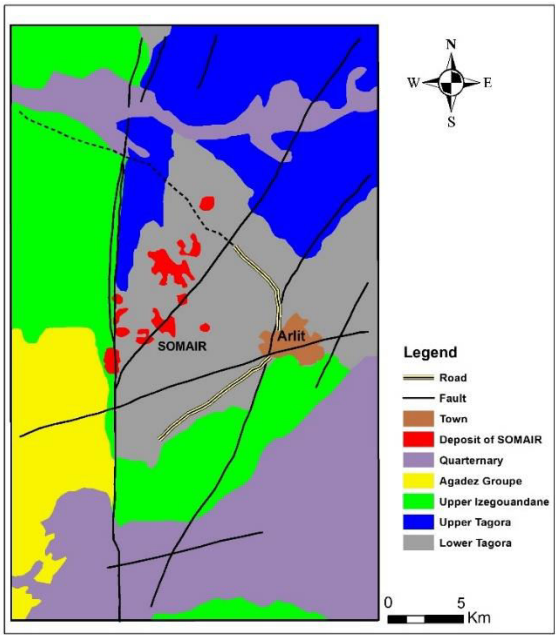

Figure.4 Structural map of northern Niger (modified from Gerbeaud, 2006)

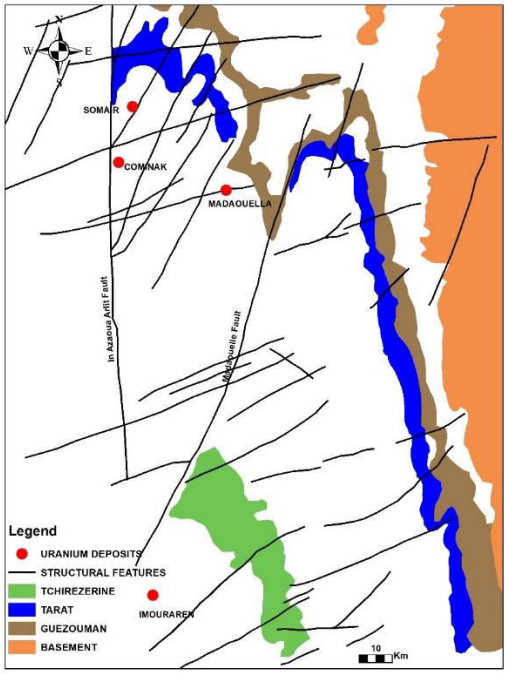

Figure.5 TMRI 420_2 lithological log

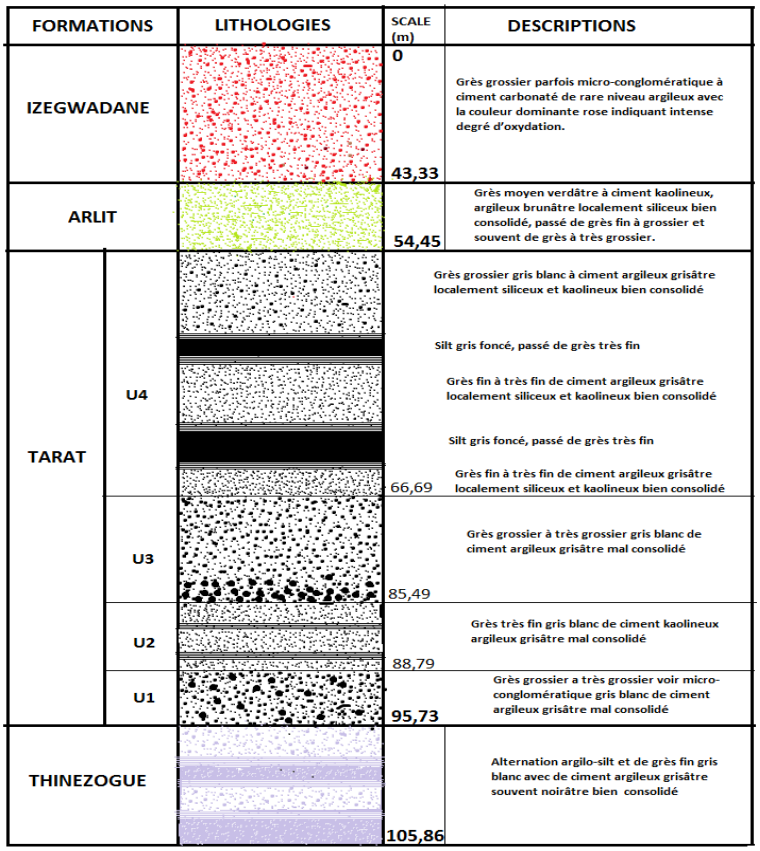

Figure.6 Lithological log with sampling numbers in Tarat

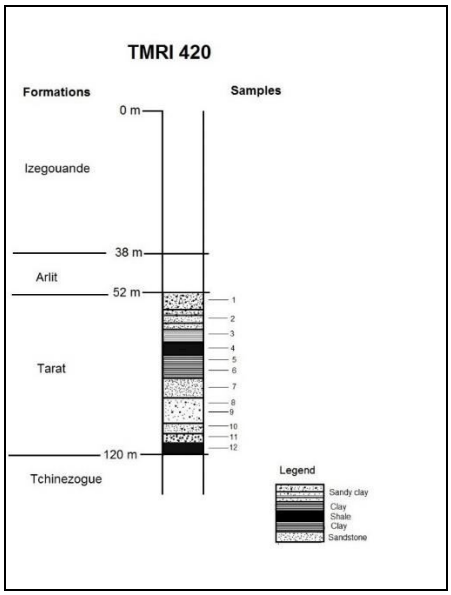

Figure.7 X-rays diffracted from the regular lattice of a perfect crystal, illustrating the conditions described by the Bragg equation. Where λ is the wavelength of rays 1 and 2, d is the spacing between planes (a and b) within the crystal lattice and θ is the acute angle between the incident ray and planes a and b, from (Nesse, 2000).

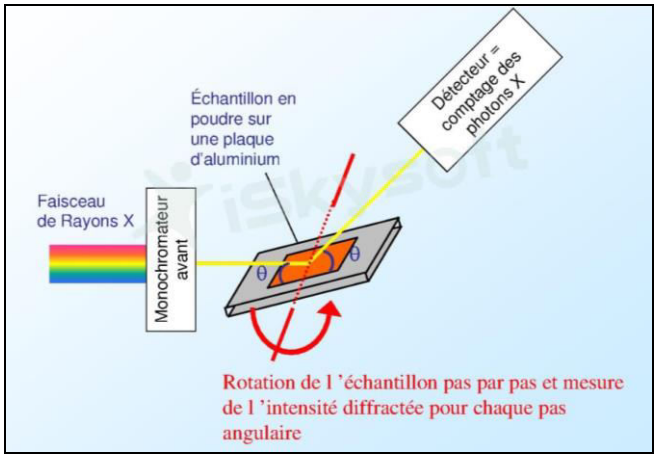

Figure.8 X-ray diffractometer.

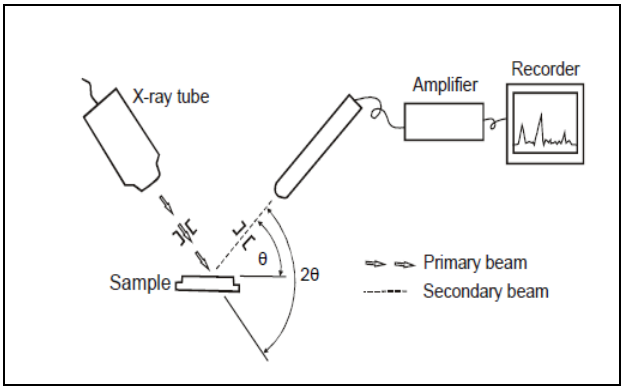

Figure.9 X-ray diffractogram (XRD) results of TMRI 420_1A and TMRI 420_2B samples

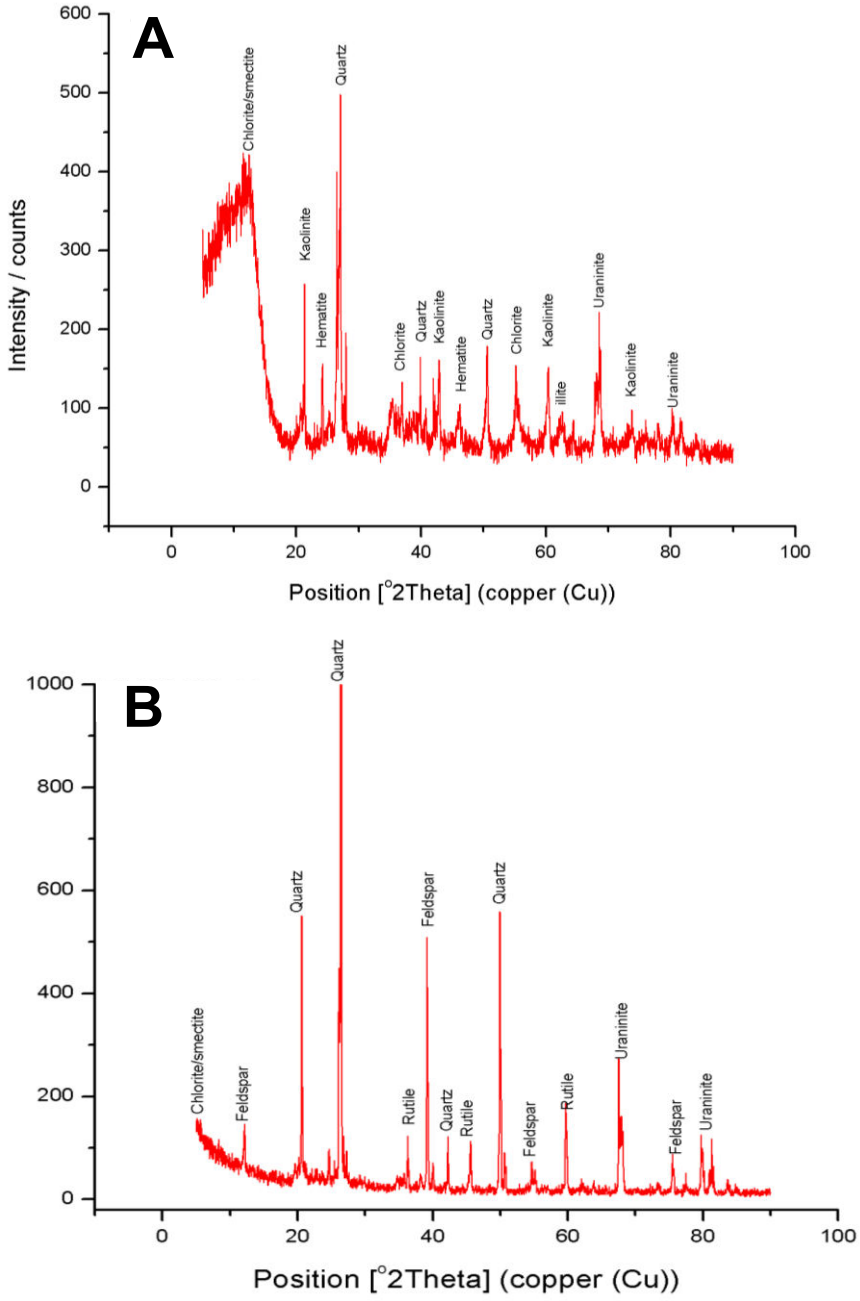

Figure.10 X-ray diffractogram (XRD) results of TMRI 420_3A and TMRI 420_4B samples

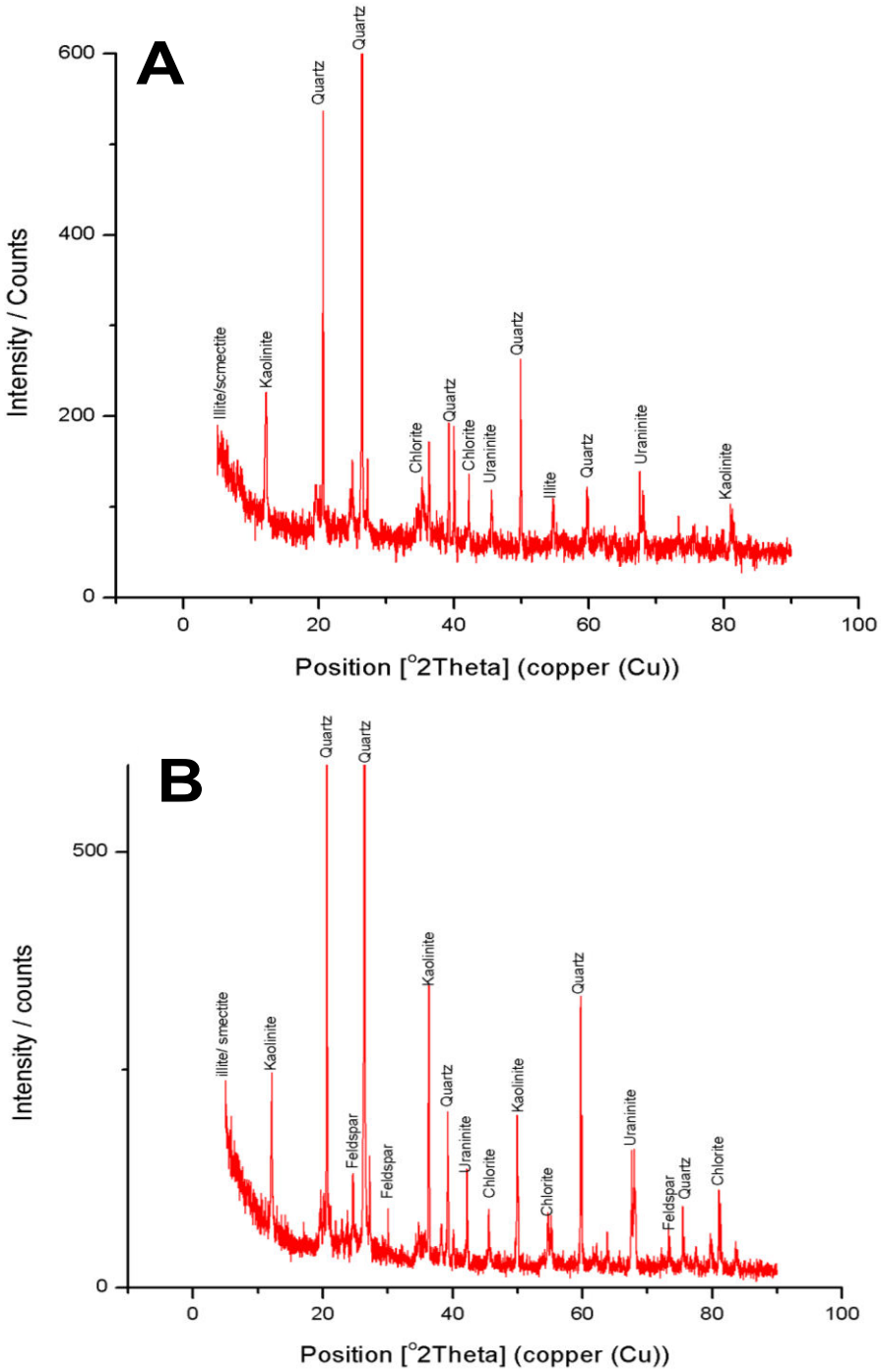

Figure.11 X-ray diffractogram (XRD) results of TMRI 420_5A and TMRI 420_6B samples

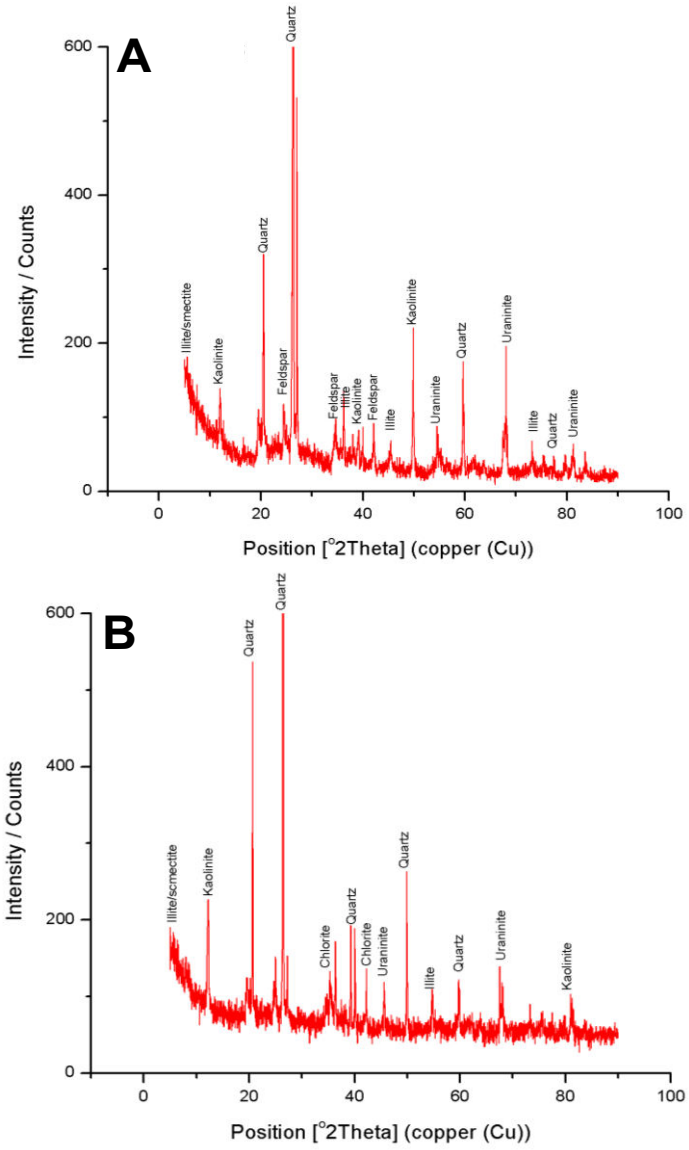

Figure.12 X-ray diffractogram (XRD) results of TMRI 420_7A and TMRI 420_8B samples

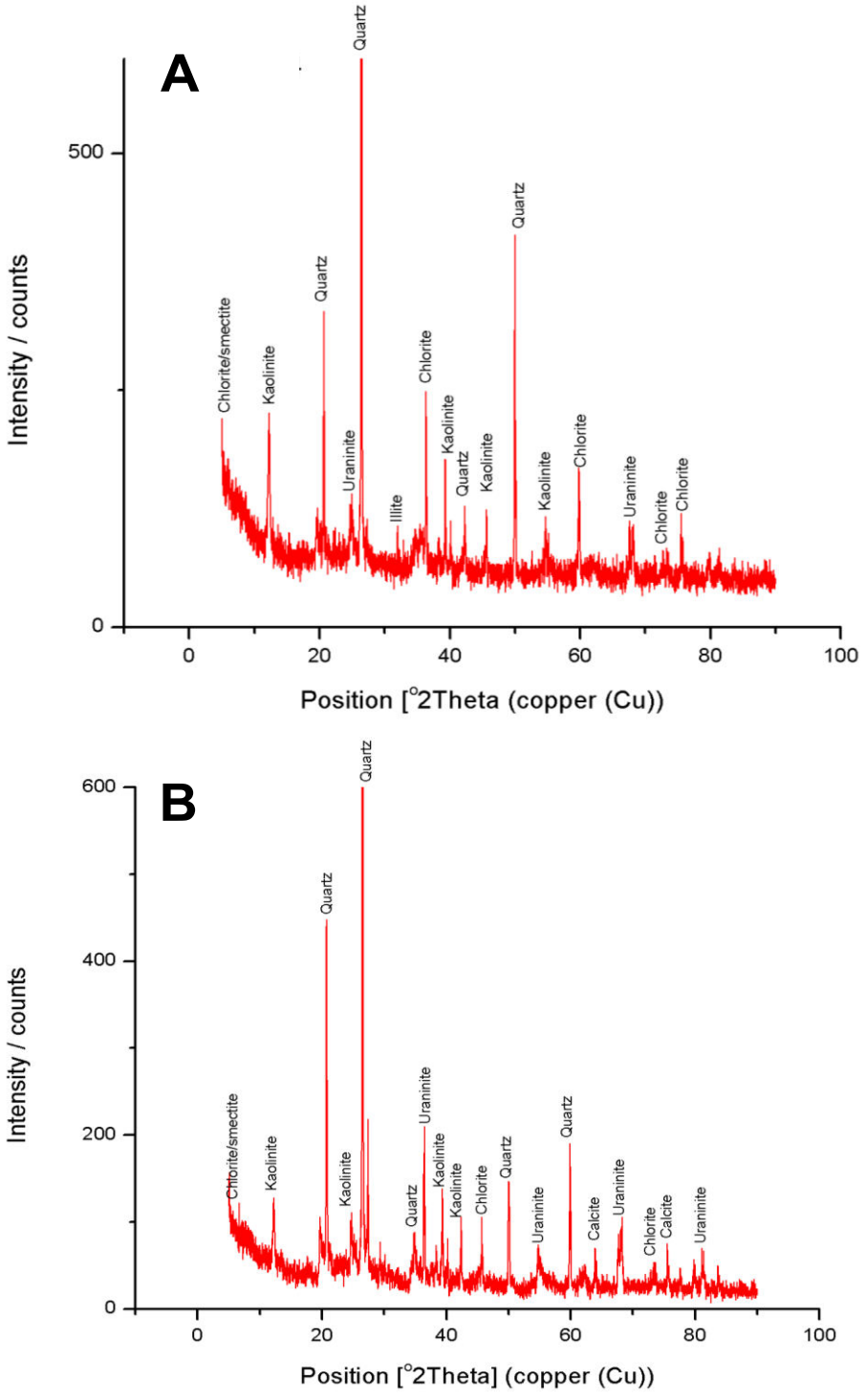

Figure.13 X-ray diffractogram (XRD) results of TMRI 420_9A and TMRI 420_10B samples

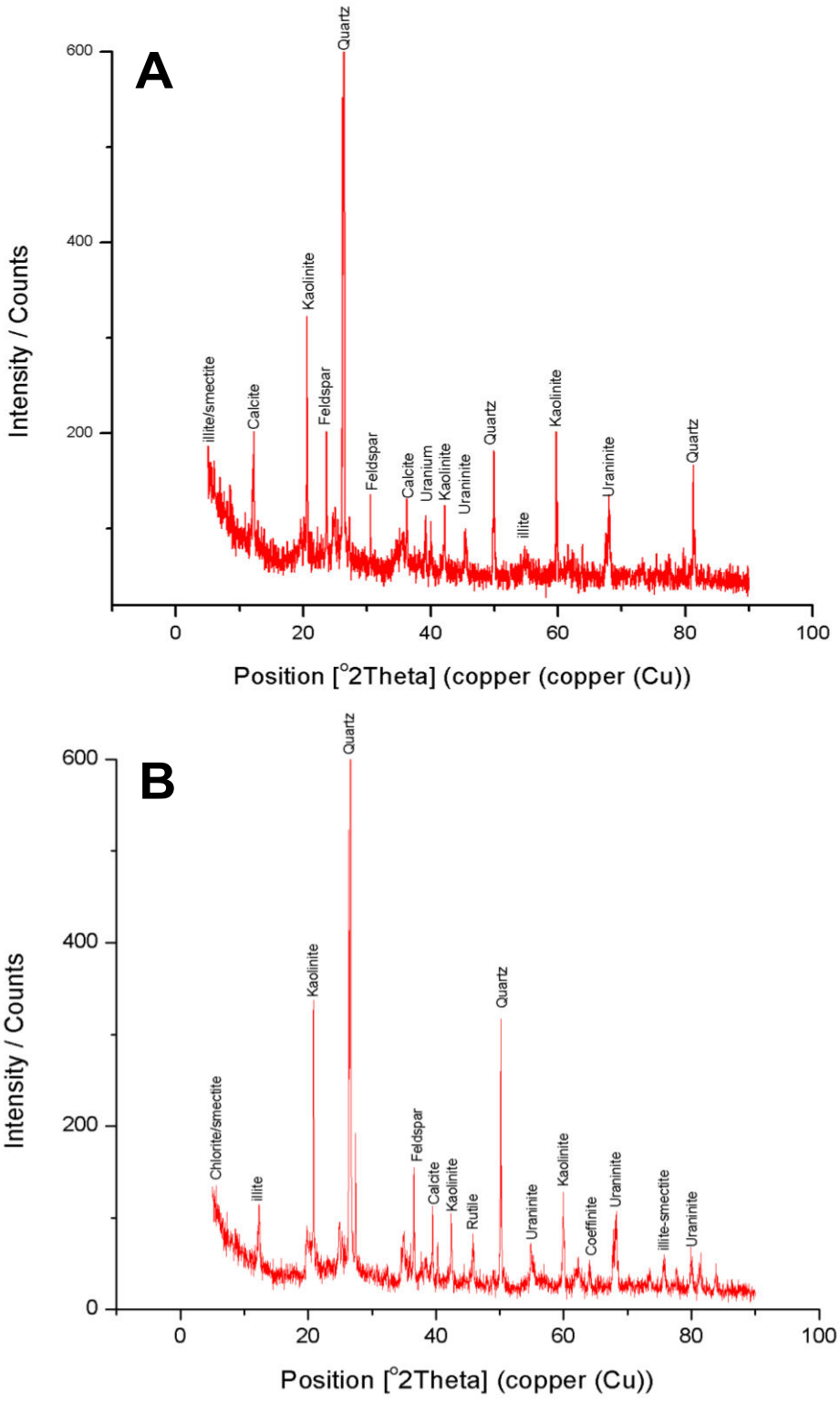

Figure.14 Projection of electron microprobe analysis data of chlorites in the Tarat formations into the 3R2-MR3-2R3 triangular diagrams.

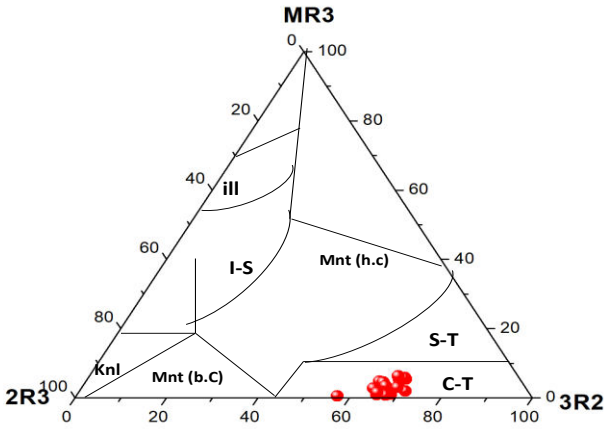

Figure.15 Classification of the different types of chlorites encountered in the Tarat formations, in the Si vs Fe/(Mg+Fe) diagram.

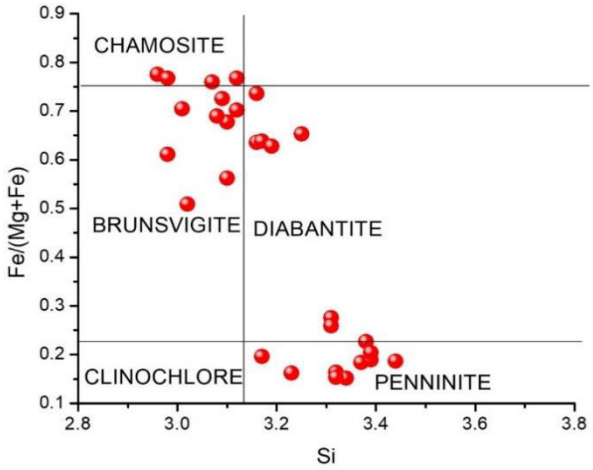

Figure.16 Variation of the composition of chlorites of the Tarat formation in the Al IV - Fe/(Fe+Mg) diagram.

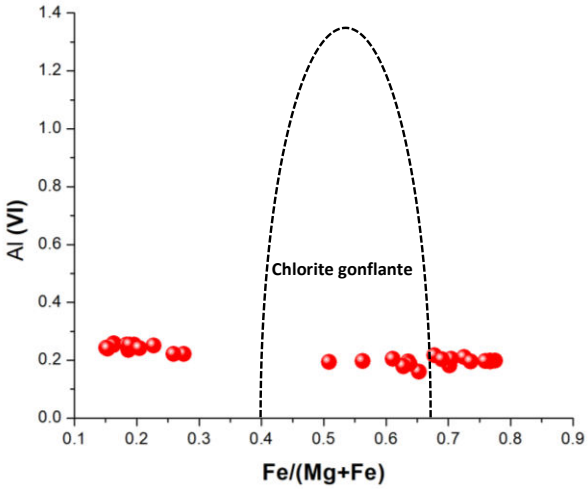

Figure.17 Position of the chlorite-smectite interstratified rocks of the Tarat Formation in the Mg - Fe - Al(VI) triangular diagram as a function of the positions of the dioctahedral corrensites and the trioctahedral corrensites.

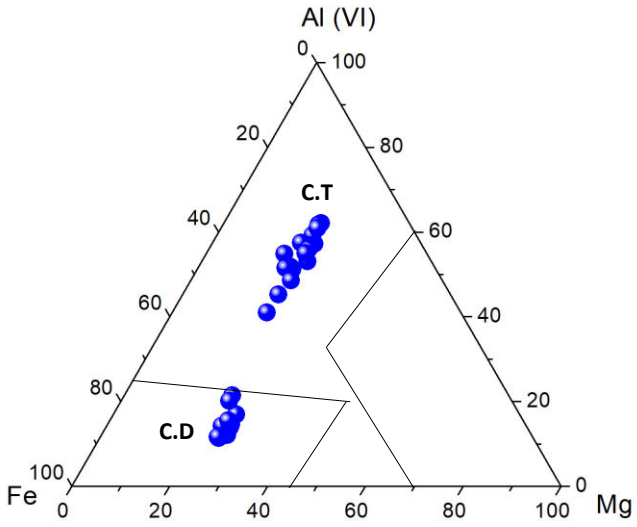

Figure.18 Projection of electron microprobe analysis data of chlorites-smectites from the Tarat Formation into the 3R2-MR3-2R3 triangular diagrams.

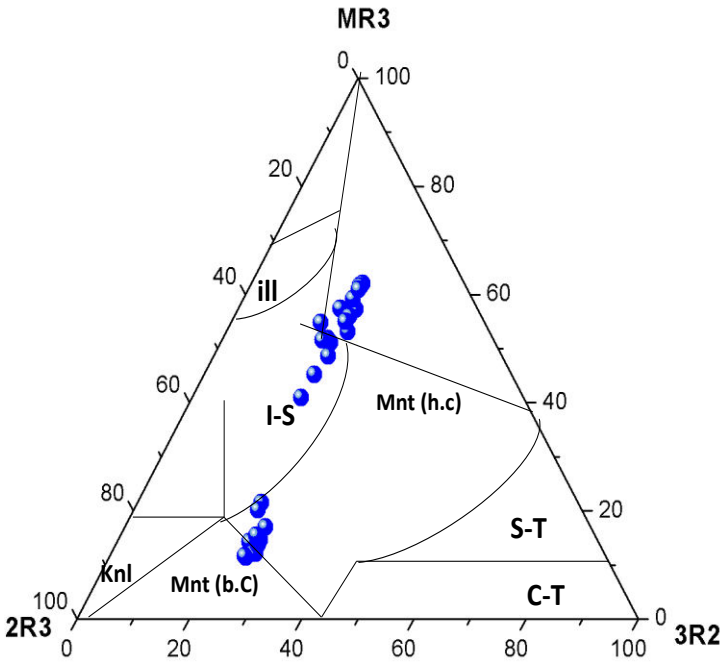

Figure.19 Projection of electron microprobe analysis data of illites from the Tarat Formation into the 3R2-MR3-2R3 triangular diagrams.

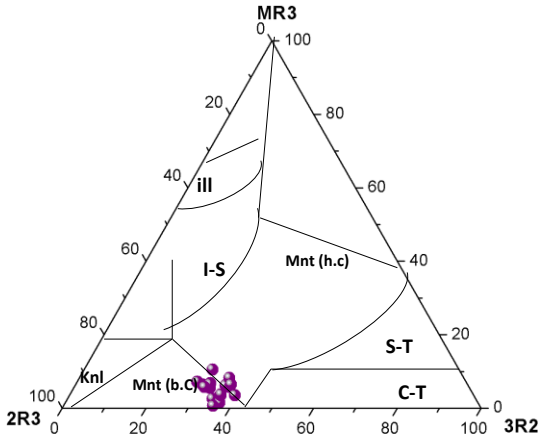

Figure.20 Projection of electron microprobe analysis data of illite-smectites from the Tarat Formation into the 3R2-MR3-2R3 triangular diagrams.

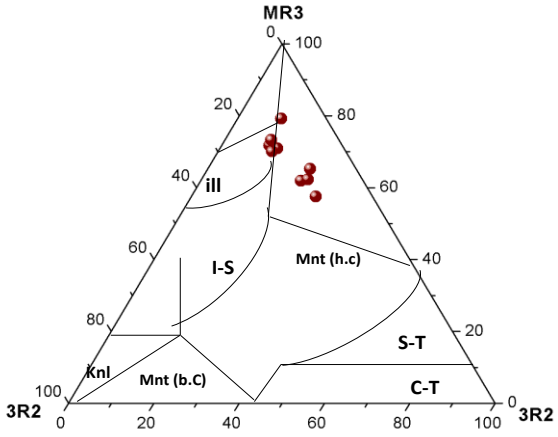

Figure.21 Projection des données analyses de microsonde électronique des kaolins de la formation du Tarat dans le diagrammes triangulaires 3R2-MR3-2R3.

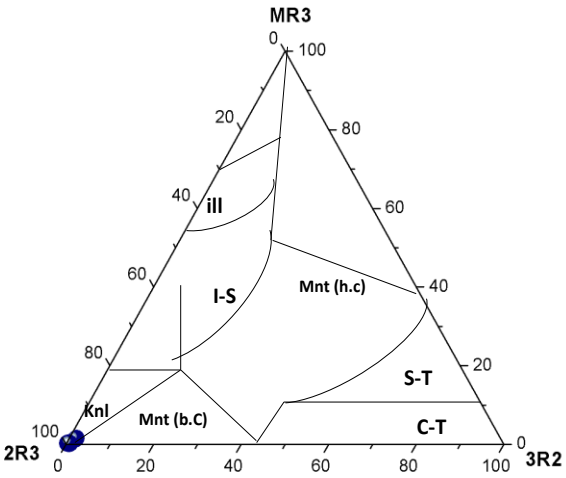

Figure.22 Lithological log with the identified minerals in Tarat

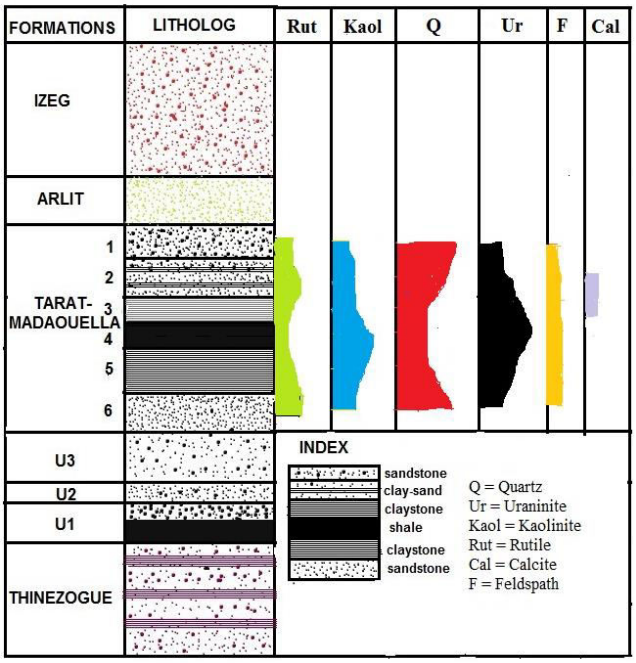

Rutile

X-ray diffraction patterns indicate the presence of rutile at the (014) and (003) lines in the diffractograms of Figures 9-13. The low presence of rutile indicates the existence of a low degree of oxidation in the Tarat formation.

Calcite

The low to very low abundance of calcite in our samples is attested by X-ray diffraction at the (114), (122) and (111) lines (Figures 9-13). Calcite is the main cement of carbonates related the low abundance of calcite is evidence of a carbonate facies.

Hématite

L'hématite a été détecté par la diffraction des rayons X (DRX) (Figure 9.1A).

Uriniferous minerals

Uranium mineralization is presented as uraninitein the Tarat formation. Uranium minerals can carry hexavalent (oxidized) or tetravalent (reduced) uranium. The total sum by weight of oxides does not add up to 100%. Several factors are mentioned to explain this low percentage by weight of oxide such as the presence of hydroxyl or hydration of Uraninite, the substitution of U4+ by U6+ or by an element not taken into account in the analysis.

Uraninite

Uraninite is identified by X-ray diffraction at the following reflections: 4.64, 3.11, 3.48, 2.789 and 2.639Å (Figures 9-13). The lithological log of the figure 22 summarize the identified minerals in the different Tarat unit.

Conclusion

The mineralogical study by X-ray diffraction of the samples of the Tarat formation allows to draw the following conclusions:

Three different groups of minerals have been identified: group of clay minerals consisting of kaolinite, chlorite and illite; group of detrital minerals composed of quartz, potassium feldspar, rutile and calcite and the group of uranium ores consisting of pitchblende;

The genesis of illite, chlorite and kaolinite is essentially detrital and were formed by the alteration of various sources of parent rocks such as acidic igneous rocks and ancient sedimentary rocks. Illite indicates a siliceous source and the low abundance of kaolinite content

testifies to the major predominance of arid climatic conditions in the initial environment of deposition.

The Tarat host formation is mineralogically composed of quartz, potassium feldspar, rutile, calcite, chlorite, illite kaolinite and pitchblende.

References

Ameh, E. S. (2019): A review of basic crystallography and X-ray diffraction applications. Int. J. Adv. Manuf. Technol, 105, 3289–3302. https://doi.org/10.1007/s00170-019-04508-1

Areva N C in Niger, (2009): Synthèse des travaux d'exploration au Niger (géologie régionale, gisements, modèles génétique, cibles) Réf. : CN/2005/R/11/AD. 23-32, 15-20.

Bailey, K.D. (1982) Methods of social research. Free Press, New York, 1982.

Billault V. (2002) - Crystal chemistry of Fe-sudoites from uranium deposits in the Athabasca basin (Saskatchewan, Canada). *Clays and Clay Minerals, 50, 69-80.*

Billault V. (2002) - Texture, structure et propriétés cristallochimiques des chlorites ferreuses dans les reservoirs gréseux. *Thèse de l'Université de Poitiers*, *197p.*

Billon, S, (2014). Minéraux argileux dans le gisement uranifère d'Imouraren (Bassin de TimMersoï, Niger) : Implications sur la genèse du gisement et sur l'optimisation des processusde traitement du minerai. Thèse de l'université de Poitiers, 340 p.

Bish, D. L. and Reynolds, R. C. (2018): Sample Preparation for X-ray Diffraction. Mod. Powder Diffr, 20, 73–100.

Bouchet, A, Meunier, A. and Sardini, P, (2000): Minéraux argileux : Structure cristalline, Identification par diffraction de rayons X, Mémoire 23. TotalFinaElf, Pau, 136 pp.

Brandt, C. G. and Kinneging, A. J, (2005). X-ray Powder Diffraction: A Practical Guide to Quantitative Phase Analysis. Panalytical, Almelo, 8

Butt, A. S (2012). Shale Characterization Using X-Ray Diffraction. Master's Thesis, Dalhousie University, Halifax, NS, Canada.

Cavellec, S, 2006. Evolution diagénétique du bassin de Tim Mersoï (district Arlit-Akokan, Niger). Thèse de l'université de Paris-Sud, 450 p

Chamley, H. (1989) Clay Sedimentology. Springer-Verlag, Berlin. https://doi.org/10.1007/978-3-642-85916-8

Claret, F, (2001): Caractérisation structurale des transitions minéralogiques dans les formations argileuses : contrôles et implications géochimiques des processus d'illitisation. Cas particulier d'une perturbation alacaline dans le Callovo-Oxfordien, Laboratoire souterrain Meuse-Haute-Marne, Université Joseph Fourrier, Grenoble, p 160.

Cullity, B. and Stock, S. (2014): Elements of X-ray Diffraction; Pearson Education Limited: New Delhi, India, 2014

Forbes P, 1983. Le gisement d'Uranium d'Akouta. Sédimentologie, Pétrographie, Minéralogie, Géochimie. Rapport CREGU, 84-02, 232 p

Gerbeaud O, (2006) : Evolution structurale du bassin de Tim Mersoï : Déformations de la couverture sédimentaire, relations avec la localisation des gisements uranifères du secteur d'Arlit (Niger). Thèse de doctorat, Université de Paris-Sud UFR scientifique d'Orsay, 270p.

Jesche, A.; Fix, M.; Kreyssig, A.; Meier, W. R.; Canfield, P. C. (2016): X-ray diffraction on large single crystals using a powder diffractometer. Philos. Mag, 96, 2115–2124. https://doi.org/10.1080/14786435.2016.1192725

Kindraich M. A, Patrier P. and Beaufort D. (2008) - Inventaire des minéraux argileux et étude cristallochimique des chlorites dans les échantillons de roches sédimentaires du gisement ďIŵouďaďeŶ; NigeďJ. *Rapport HydrASA, Université de Poitiers, 35p*

Kogbe. C. A, (1991): Stratigraphy and tectonic history of the Iullemeden Basin in west Africa. S. Afr. J. Geol. 94 (1), 19 - 31.

Mamane, (2016). "Le Système Métallogénique Des Gisements d'uranium Associes à` La Faille d'Arlit (Bassin de Tim Mersoï, Niger) : Diagenèse, Circulations Des Fluides et mécanismes d'enrichissement En métaux (U, Cu, V) Soutenance."

Matsubara, E.; Shinoda, K.; Waseda, Y (2011): X-ray Diffraction Crystallography: Introduction, Examples and Solved Problems; Springer: Berlin/Heidelberg, Germany.

Millot, G. (1964) Géologie des argiles. Masson et Cie Ed., Paris, 499.

Moore, D. M. and Reynolds, R. C, (1989): X-ray Diffraction and the Identification and Analysis of Clay Minerals. Oxford University Press, 322 pp.

Nesse, W. D, (2000): *Introduction to Mineralogy*. Oxford University Press. New York, 163.

Pacquet, A, 1969. Analcimes et argiles diagénétiques dans les formations sédimentaires de la région d'Agadès (République du Niger. Thèse de l'université de Strasbourg, 258 p

Plançon, A. and Drits, V. A, (2000): Phase analysis of clays using an expert system and calculation programs for X ray diffraction by two- and three-component mixed-layer minerals. Clays and Clay Minerals, 48(1): 57-62. http://dx.doi.org/10.1346/CCMN.2000.0480107

Rigault C. (2010) - Cristallochimie du fer dans les chlorites de basse température : implications pour la géothermométrie et la détermination des paléoconditions rédox dans les gisements d'uranium. *Thèse de l'Université de Poitiers, 259p.*

Tucker, M, (1988): Techniques in Sedimentology. Blackwell Scientific Publications. Oxford 0X2 OEL 8 John Street.

Tucker, M, (1991): Sedimentary Petrology: An introduction to the origin of Sedimentary rocks. Blackwell Scientific Publications. Oxford OX2 OEL 8 John Street.

Turpin. L, Clauer N, Forbes. P, and Pagel. M, (1991): U-Pb, Sm-Nd and K-Ar systematic of the Akouta Uranium deposit, Niger. Chemical Geology 87, 217 – 230. https://doi.org/10.1016/0168-9622(91)90022-O

Velde B. (1985) - Clay Minerals: A Physic-Chemical Explanation of their Occurrence. *Elsevier, Amsterdam, 427p.*

Velde, B. (1995) Composition and Mineralogy of Clay Minerals. In: Velde. B., Ed., Origin and Mineralogy of Clays: Clays and the Environment, Springer, Berlin, 8-42. https://doi.org/10.1007/978-3-662-12648-6_2

Waseda, Y., E. Matsubara and K. Shinoda (2011): X-Ray Diffraction Crystallography: Introduction, Examples and Solved Problems. https://doi.org/10.1007/978-3-642-16635-8

How to cite this article:

Tourba Kamayé, Abdou Dodo Bohari, Ibrahim Sarki Laouali, Ibrahim Hassan Mahrou, Mallam Maman Halarou, Hamma Ada Moussa and Moussa Harouna. 2024. Application of X-Ray Diffraction for Mineralogical Composition Studies of Tarat Formation Sandstone in the Tamari Prospect, Northern Niger. *Int.J.Curr.Res.Aca.Rev.* 12(11), 38-55. doi: https://doi.org/10.20546/ijcrar.2024.1211.002